Optimization and Acceleration Guidance of Flight Trajectories in a Windshear

A. Miele* and T. Wang†
Rice University, Houston, Texas
and
W. W. Melvin‡
Delta Airlines, Atlanta, Georgia

This paper is concerned with guidance strategies for near-optimum performance in a windshear. The takeoff problem is considered with reference to flight in a vertical plane. In addition to the horizontal shear, the presence of a downdraft is assumed. First, trajectories for optimum performance in a windshear are determined for different windshear models and intensities. Use is made of the methods of optimal control theory in conjunction with the dual sequential gradient-restoration algorithm (DSGRA) for optimal control problems. In this approach, global information on the wind flowfield is needed. Then, guidance strategies for near-optimum performance in a windshear are developed, starting from the optimal trajectories. Specifically, an acceleration guidance scheme based on the relative acceleration is presented in both analytical and feedback control forms. In this approach, local information on the wind flowfield is needed. Numerical experiments show that the acceleration guidance scheme produces trajectories that are quite close to the optimum trajectories. In addition, the near-optimum trajectories are superior to the trajectories arising from alternative guidance schemes. An important characteristic of the acceleration guidance scheme is its simplicity. Indeed, this guidance scheme is implementable if local information on the windshear, the downdraft, and the state of the aircraft is available.

Nomenclature

ARL = aircraft reference line
C_D = drag coefficient
C_L = lift coefficient
D = drag force, lb
g = acceleration of gravity, ft s^{-2}
h = altitude, ft
K = gain coefficient
L = lift force, lb
m = mass, lb $ft^{-1}s^2$
S = reference surface, ft^2
T = thrust force, lb
V = relative velocity, ft s^{-1}
V_e = absolute velocity, ft s^{-1}
W = mg = weight, lb
W = wind velocity, ft s^{-1}
W_h = h-component of wind velocity, ft s^{-1}
W_x = x-component of wind velocity, ft s^{-1}
x = horizontal distance, ft
α = relative angle of attack, rad
α_e = absolute angle of attack, rad
β = engine power setting
γ = relative path inclination, rad
γ_e = absolute path inclination, rad
δ = thrust inclination, rad
θ = pitch attitude angle, rad
ρ = air density, lb $ft^{-4}s^2$

Received June 16, 1986; presented as Paper 86-2036 at the AIAA Guidance, Navigation, and Control Conference, Williamsburg, VA, Aug. 18–20, 1986; revision submitted Nov. 10, 1986.

*Professor of Astronautics and Mathematical Sciences, Aero-Astronautics Group. Fellow AIAA.
†Senior Research Associate, Aero-Astronautics Group.
‡Captain and Chairman, Airworthiness and Performance Committee, Air Line Pilots Association (ALPA), Washington, DC.

I. Introduction

LOW-altitude windshear constitutes a considerable hazard in the takeoff and landing of both civilian and military airplanes. For this reason, considerable research has been done on this problem over the past fifteen years. Most of the research has been concerned with meteorology, instrumentation, aerodynamics, flight mechanics, and stability and control. Recently, optimal flight trajectories in the presence of a windshear have been studied (Refs. 2–4). This opens the road to the development of guidance schemes for achieving near-optimum performance in a windshear (Refs. 5 and 6).

Previous Research

Previous research on the topics covered in this paper can be found in Refs. 7–25. For a general review of windshear studies, see Ref. 7. For the equations of motion without windshear, see Ref. 8; for the equations of motion with windshear, see Ref. 9 and Ref. 2, Part 1. For windshear models, see Refs. 10–12.

Concerning trajectory optimization, for a recent overview of theoretical calculus of variations and optimal control, see Ref. 13. For algorithmic optimal control by means of gradient methods, see Refs. 14 and 15 (primal formulation) and Refs. 16 and 17 (dual formulation). For minimax optimal control, see Refs. 18 and 19. Finally, for additional studies of control, optimization, and guidance of flight trajectories in a windshear, see Refs. 20–25.

Present Research

This paper is concerned with guidance schemes for near-optimum performance in a windshear. In addition to the horizontal shear, the presence of a downdraft is assumed. Note that the downdraft had been neglected in Refs. 2–6.

The takeoff problem is considered with reference to flight in a vertical plane. In takeoff, once an aircraft becomes airborne, the pilot has no choice but to fly through a windshear. His only control is the angle of attack. Indeed, it is logical to assume that, if a plane takes off under less than ideal weather

conditions, the power setting is being held at that value which yields the maximum thrust.

First, trajectories for optimum performance in a windshear are determined for different windshear models and intensities. In this approach, global information on the wind flowfield is needed. Then, guidance schemes for near-optimum performance in a windshear are developed, starting from the optimal trajectories. Specifically, an acceleration guidance scheme based on the relative acceleration is presented in both analytical and feedback control forms. In this approach, local information on the wind flowfield is needed. Next, the acceleration guidance scheme is evaluated through numerical experiments in order to 1) determine whether the resulting trajectories are sufficiently close to the optimum trajectories and 2) compare the resulting trajectories with those arising from alternative guidance schemes.

II. Formulation of the Problem

A. Equations of Motion

In this paper, we make use of the relative wind axes system (Fig. 1) in connection with the following assumptions: (1) the aircraft is a particle of constant mass, (2) flight takes place in a vertical plane, (3) Newton's law is valid in an Earth-fixed system, and (4) the wind flowfield is steady. With these premises, the equations of motion include the kinematical equations

$$\dot{x} = V\cos\gamma + W_x \tag{1a}$$

$$\dot{h} = V\sin\gamma + W_h \tag{1b}$$

and the dynamical equations

$$\dot{V} = (T/m)\cos(\alpha+\delta) - D/m - g\sin\gamma - (\dot{W}_x\cos\gamma + \dot{W}_h\sin\gamma) \tag{2a}$$

$$\dot{\gamma} = (T/mV)\sin(\alpha+\delta) + L/mV - (g/V)\cos\gamma + (1/V)(\dot{W}_x\sin\gamma - \dot{W}_h\cos\gamma) \tag{2b}$$

Because of the fourth assumption, the total derivatives of the wind velocity components and the corresponding partial derivatives satisfy the relations

$$\dot{W}_x = (\partial W_x/\partial x)(V\cos\gamma + W_x) + (\partial W_x/\partial h)(V\sin\gamma + W_h) \tag{3a}$$

$$\dot{W}_h = (\partial W_h/\partial x)(V\cos\gamma + W_x) + (\partial W_h/\partial h)(V\sin\gamma + W_h) \tag{3b}$$

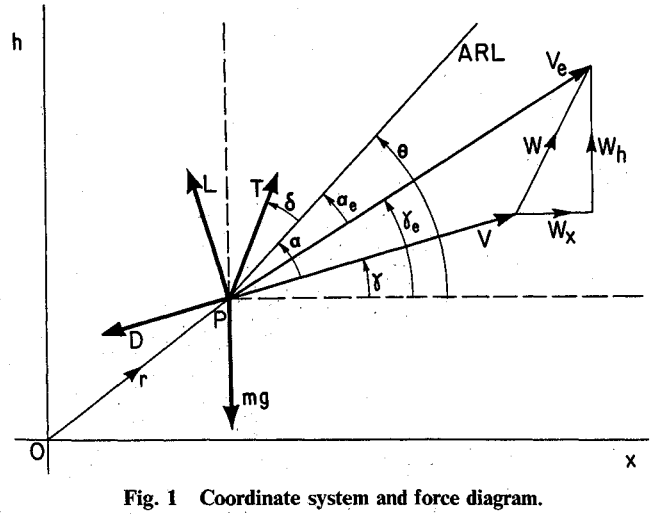

Fig. 1 Coordinate system and force diagram.

As a consequence, the dynamical equations can be rewritten in the form

$$\dot{V} = (T/m)\cos(\alpha+\delta) - D/m - g\sin\gamma - [(\partial W_x/\partial x)(V\cos\gamma + W_x) + (\partial W_x/\partial h)(V\sin\gamma + W_h)]\cos\gamma - [(\partial W_h/\partial x)(V\cos\gamma + W_x) + (\partial W_h/\partial h)(V\sin\gamma + W_h)]\sin\gamma \tag{4a}$$

$$\dot{\gamma} = (T/mV)\sin(\alpha+\delta) + L/mV - (g/V)\cos\gamma + [(\partial W_x/\partial x)(V\cos\gamma + W_x) + (\partial W_x/\partial h)(V\sin\gamma + W_h)](1/V)\sin\gamma - [(\partial W_h/\partial x)(V\cos\gamma + W_x) + (\partial W_h/\partial h)(V\sin\gamma + W_h)](1/V)\cos\gamma \tag{4b}$$

These equations must be supplemented by the functional relations

$$T = T(h, V, \beta) \tag{5a}$$

$$D = D(h, V, \alpha), \qquad L = L(h, V, \alpha) \tag{5b}$$

$$W_x = W_x(x, h), \qquad W_h = W_h(x, h) \tag{5c}$$

and by the analytical relations

$$V_{ex} = V\cos\gamma + W_x, \qquad V_{eh} = V\sin\gamma + W_h \tag{6a}$$

$$V_e = \sqrt{(V_{ex}^2 + V_{eh}^2)}, \qquad \gamma_e = \arctan(V_{eh}/V_{ex}) \tag{6b}$$

$$\theta = \alpha + \gamma, \qquad \alpha_e = \alpha + \gamma - \gamma_e \tag{6c}$$

For a given value of the thrust inclination δ, the differential system of Eqs. (1), (4), and (5) involves four state variables [the horizontal distance $x(t)$, the altitude $h(t)$, the velocity $V(t)$, and the relative path inclination $\gamma(t)$] and two control variables [the angle of attack $\alpha(t)$ and the power setting $\beta(t)$]. However, the number of control variables reduces to one (the angle of attack α) if the power setting β is specified in advance. The quantities defined by the analytical relations (6) can be computed a posteriori once the values of x, h, V, γ, α, and β are known.

B. Inequality Constraints

The angle of attack α and its time derivative $\dot{\alpha}$ are subject to the inequalities

$$\alpha \le \alpha_* \tag{7a}$$

$$-C \le \dot{\alpha} \le +C \tag{7b}$$

where α_* is a prescribed upper bound and C is a prescribed positive constant. For the optimal trajectories of Sec. III, Ineqs. (7) are satisfied indirectly via transformation techniques converting the inequality constraints into equality constraints (see Ref. 2, Part 2), specifically,

$$\alpha = \alpha_* - u^2 \tag{8a}$$

$$\dot{u} = -(C/2u)\sin w, \qquad |u| \ge \epsilon \tag{8b}$$

$$\dot{u} = -(C/2u)\sin^2(\pi u/2\epsilon)\sin w, \qquad |u| \le \epsilon \tag{8c}$$

Here, $u(t)$ and $w(t)$ are auxiliary variables and ϵ is a small, positive constant introduced to prevent the occurrence of singularities. Incidentally, the right-hand sides of Eqs. (8b) and (8c) are continuous and have continuous first derivatives at $|u| = \epsilon$.

For the guidance schemes of Sec. IV, Ineq. (7a) is satisfied directly. On the other hand, Ineq. (7b) is satisfied indirectly through the proper choice of the gain coefficient K.

C. Approximations for the Force Terms

In this section, we discuss the approximations employed for the thrust, the drag, the lift, and the weight. Because the trajectories under investigation involve relatively minor variations of the altitude, the air density is assumed to be constant.

The thrust T is approximated with the quadratic function

$$T = A_0 + A_1 V + A_2 V^2 \tag{9}$$

where V is the relative velocity. The coefficients A_0, A_1, and A_2 depend on the altitude of the runway, the ambient temperature, and the engine power setting.

The drag D is written in the form

$$D = (1/2) C_D \rho S V^2 \tag{10a}$$

$$C_D = B_0 + B_1 \alpha + B_2 \alpha^2, \qquad \alpha \leq \alpha_* \tag{10b}$$

where ρ is the air density, S is a reference surface, V is the relative velocity, and C_D is the drag coefficient. The coefficients B_0, B_1, and B_2 depend on the flap setting and the undercarriage position (gear up or gear down).

The lift L is written in the form

$$L = (1/2) C_L \rho S V^2 \tag{11a}$$

$$C_L = C_0 + C_1 \alpha, \qquad \alpha \leq \alpha_{**} \tag{11b}$$

$$C_L = C_0 + C_1 \alpha + C_2 (\alpha - \alpha_{**})^2, \qquad \alpha_{**} \leq \alpha \leq \alpha_* \tag{11c}$$

where ρ is the air density, S is a reference surface, V is the relative velocity, and C_L is the lift coefficient. The coefficients C_0, C_1, and C_2 depend on the flap setting and the undercarriage position (gear up or gear down).

The mass m is regarded as constant. Hence, the weight $W = mg$ is regarded as constant.

D. Approximations for the Windshear

We refer to the meteorological condition known as a microburst. This condition involves a descending column of air that spreads horizontally in the neighborhood of the ground. This condition is hazardous because an aircraft in takeoff or landing might encounter a headwind coupled with a downdraft, followed by a tailwind coupled with a downdraft. A qualitative example of the vertical cross section of a microburst is shown in Fig. 2.

Under the assumption that the wind flowfield is steady, the wind components W_x, W_h have the form (5c). From an engineering point of view, a further simplifying observation can be made. Because takeoff trajectories involve relatively minor variations of the altitude, the wind components W_x, W_h can be assumed to depend only on the horizontal distance. Within this frame, three different windshear models are considered here:

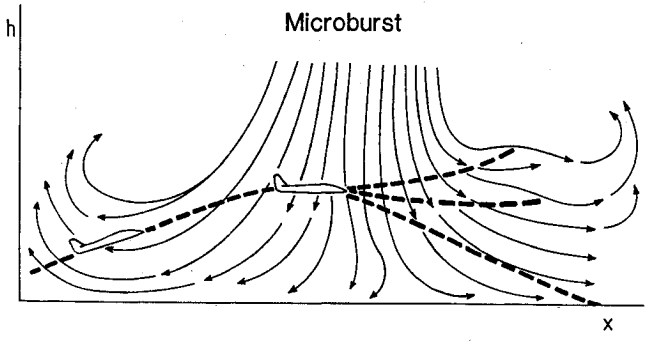

Fig. 2 Microburst encounter.

$$\text{(WS1)} \quad W_x = W_x(x), \qquad W_h = 0 \tag{12a}$$

$$\text{(WS2)} \quad W_x = 0, \qquad W_h = W_h(x) \tag{12b}$$

$$\text{(WS3)} \quad W_x = W_x(x), \qquad W_h = W_h(x) \tag{12c}$$

Windshear model WS1 includes the horizontal shear and neglects the downdraft. Windshear model WS2 is complementary to WS1 in that it neglects the horizontal shear and includes the downdraft. Finally, windshear model WS3 generalizes WS1 and WS2 in that it includes both the horizontal shear and the downdraft.

Obviously, windshear model WS3 is closer to reality than windshear models WS1 and WS2. However, the study of the behavior of an aircraft under models WS1 and WS2 is important to the construction of a guidance scheme, since models WS1 and WS2 represent two extreme cases.

III. Optimal Flight Trajectories

A. Optimal Control Problem

We refer to takeoff trajectories and assume that global information on the wind flowfield is available, that is, that Eqs. (5c) are known in advance, the power setting $\beta(t)$ is given, and the angle of attack $\alpha(t)$ is subject to Ineqs. (7). Hence, upon converting the inequalities into equalities, we refer to the differential system described by Eqs. (1), (4), (5), and (8). In this system, the state variables are $x(t)$, $h(t)$, $V(t)$, $\gamma(t)$, $\alpha(t)$, and $u(t)$ and the control variable is $w(t)$. We formulate the following optimization problem.

Problem (P)

Subject to the previous constraints, minimize the peak value of the modulus of the difference between the absolute path inclination and a reference value, assumed constant. In this problem, the performance index is given by

$$I = \max_t |\gamma_e - \gamma_{eR}|, \qquad 0 \leq t \leq \tau \tag{13a}$$

where

$$\gamma_e = \arctan[(V \sin\gamma + W_h)/(V \cos\gamma + W_x)] \tag{13b}$$

$$\gamma_{eR} = \gamma_{e0} \tag{13c}$$

This is a minimax problem or Chebyshev problem of optimal control. It can be reformulated as a Bolza problem of optimal control (Ref. 19), in which one minimizes the integral performance index

$$J = \int_0^\tau (\gamma_e - \gamma_{eR})^q \, dt \tag{13d}$$

for large values of the positive even exponent q.

B. Boundary Conditions

Concerning the initial conditions, it is assumed that the values of x, h, V, γ, and α are specified at $t = 0$, that is,

$$x(0) = x_0, \qquad h(0) = h_0, \qquad V(0) = V_0 \tag{14a}$$

$$\gamma(0) = \gamma_0, \qquad \alpha(0) = \alpha_0 \tag{14b}$$

Upon combining Eqs. (8a) and (14b), we see that the specification of the initial value of α implies the specification of the initial value of u, that is,

$$u(0) = u_0 = \sqrt{(\alpha_* - \alpha_0)} \tag{14c}$$

Concerning the final conditions, it is assumed that the value of γ is specified at $t=\tau$, that is,

$$\gamma(\tau)=\gamma_0 \tag{15}$$

The remaining state variables are free at the final point. The final time τ is chosen to be large enough to correspond to a no-windshear condition. Clearly, the use of Eq. (15) means that at the final point one intends to achieve gamma recovery, namely, to restore the initial value of the relative path inclination.

C. Sequential Gradient-Restoration Algorithm

Problem (P), governed by Eqs. (1), (4), (5), (8), and (13–15), is a Bolza problem of optimal control. It can be solved using the family of sequential gradient-restoration algorithms for optimal control problems (SGRA, Refs. 14–17) in either the primal formulation (PSGRA, Refs. 14 and 15) or the dual formulation (DSGRA, Refs. 16 and 17).

Regardless of whether the primal formulation or dual formulation is used, sequential gradient-restoration algorithms involve a sequence of two-phase cycles, each cycle including a gradient phase and a restoration phase. In the gradient phase, the value of the augmented functional is decreased, while avoiding excessive constraint violation. In the restoration phase, the value of the constraint error is decreased, while avoiding excessive change in the value of the functional. In a complete gradient-restoration cycle, the value of the functional is decreased, while the constraints are satisfied to a preselected degree of accuracy. Thus, a succession of suboptimal solutions is generated, each new solution being an improvement over the previous one from the point of view of the value of the functional being minimized.

The convergence conditions are represented by the relations

$$P\leq\epsilon_1, \qquad Q\leq\epsilon_2 \tag{16}$$

Here, P is the norm squared of the error in the constraints, Q is the norm squared of the error in the optimality conditions, and ϵ_1 and ϵ_2 are preselected small positive numbers.

In this work, the sequential gradient-restoration algorithm is employed in conjunction with the dual formulation. The algorithmic details can be found in Refs. 16 and 17. They are omitted here for the sake of brevity.

D. Data for the Examples

Aircraft

The aircraft under consideration is a Boeing B-727 aircraft powered by three JT8D-17 turbofan engines. It is assumed that the aircraft has become airborne from a runway located at sea-level altitude, the ambient temperature is 100° F, the gear is up, the flap setting is $\delta_F=15$ deg, the engines are operating at maximum power setting, and the takeoff weight is $W=180{,}000$ lb.

Complete data for this aircraft are omitted here for the sake of brevity; they can be found in Ref. 2, Part 4. It is of interest to note that the maximum lift-to-drag ratio of this configuration is $(L/D)_{\max}=10.52$ and that the average thrust-to-weight ratio over the velocity interval of interest is $(T/W)_{av}=0.22$.

Windshear Models

Three windshear models are considered. They are described by Eqs. (12) and are shown in Fig. 3.

Windshear model WS1 has the form (12a); it includes the horizontal shear and neglects the downdraft. The function $W_x(x)$ represents a linear transition from a uniform headwind of -40 ft s^{-1} to a uniform tailwind of $+40$ ft s^{-1}; hence, the wind velocity difference is $\Delta W_x=80$ ft s^{-1}. The transition takes place over a distance $\Delta x=4000$ ft, starting at $x=300$ ft and ending at $x=4300$ ft; hence, the average wind gradient is $\Delta W_x/\Delta x=0.020$ s^{-1}.

Windshear model WS2 has the form (12b); it is complementary to model WS1 in that it neglects the horizontal shear and includes the downdraft. The function $W_h(x)$ has a bell-shaped form; in particular, the downdraft vanishes at $x=300$ and 4300 ft and achieves the maximum negative value of -20 ft s^{-1} at $x=2300$ ft; hence, $\Delta W_h=20$ ft s^{-1}.

Windshear model WS3 has the form (12c); it generalizes models WS1 and WS2 in that it includes both the horizontal shear and the downdraft. The function $W_x(x)$ is the same as in model WS1; the function $W_h(x)$ is the same as in model WS2.

To sum up, windshear models WS1, WS2, and WS3 are characterized by the following values of $\Delta W_x, \Delta W_h$:

$$\text{(WS1)} \quad \Delta W_x=80 \text{ ft s}^{-1}, \qquad \Delta W_h=0 \text{ ft s}^{-1} \tag{17a}$$

$$\text{(WS2)} \quad \Delta W_x=0 \text{ ft s}^{-1}, \qquad \Delta W_h=20 \text{ ft s}^{-1} \tag{17b}$$

$$\text{(WS3)} \quad \Delta W_x=80 \text{ ft s}^{-1}, \qquad \Delta W_h=20 \text{ ft s}^{-1} \tag{17c}$$

Inequality Constraints

The angle of attack and its time derivative are subject to Ineqs. (7), with

$$\alpha_*=16 \text{ deg}, \qquad C=3 \text{ deg s}^{-1} \tag{18a}$$

The constant ϵ in Eqs. (8) is set at the level

$$\epsilon=0.4 \tag{18b}$$

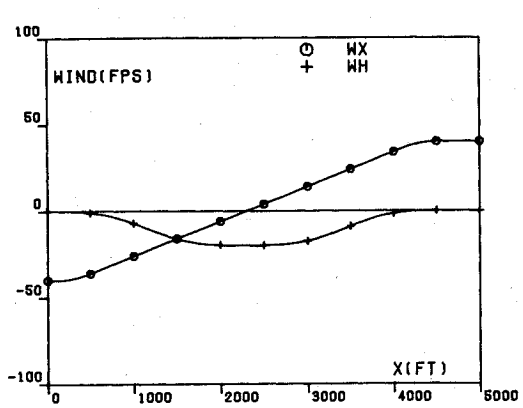

Fig. 3a Wind velocity components W_x, W_h vs horizontal distance x.

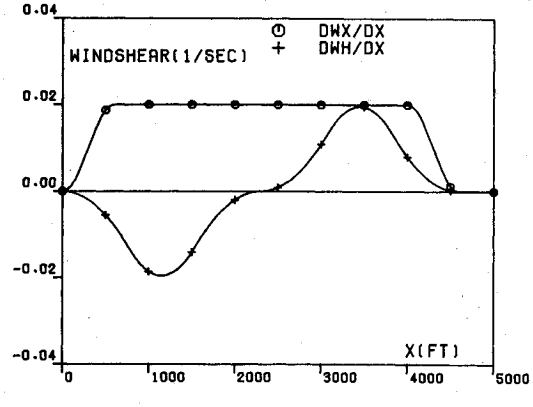

Fig. 3b Gradients of wind velocity components $\partial W_x/\partial x$, $\partial W_h/\partial x$ vs horizontal distance x.

Initial Conditions

The following initial conditions are assumed:

$$x(0) = 0 \text{ ft}, \qquad h(0) = 50 \text{ ft} \tag{19a}$$

$$V(0) = 276.8 \text{ ft s}^{-1}, \qquad \gamma(0) = 6.989 \text{ deg} \tag{19b}$$

$$\alpha(0) = 10.36 \text{ deg} \tag{19c}$$

We note that these values correspond to quasi-steady flight and the initial velocity $V(0)$ is FAA certification velocity V_2, augmented by 10 knots; in turn, the velocity $V_2 + 10$ (in knots) corresponds approximately to the steepest climb condition in quasi-steady flight.

Final Conditions

To achieve gamma recovery, it is required that

$$\gamma(\tau) = 6.989 \text{ deg} \tag{20}$$

The final time is set at the value

$$\tau = 40 \text{ s} \tag{21}$$

This is about twice the duration of the windshear encounter ($\Delta t = 18$ s).

Performance Index

The numerical constants appearing in the performance indexes I and J of Problem (P) are given here:

$$\gamma_{eR} = 8.165 \text{ deg}, \qquad q = 6 \tag{22}$$

E. Numerical Results

Problem (P), minimax $|\Delta\gamma_e|$, was solved with the sequential gradient-restoration algorithm employed in conjunction with the dual formulation (DSGRA, Refs. 16 and 17). Computations were performed at Rice University using an NAS-AS-9000 computer.

For computational efficiency, the state variables and the time were suitably scaled. For Problem (P), the functional being minimized was suitably scaled. The following stopping conditions were employed for the dual sequential gradient-restoration algorithm:

$$P \leq E-10, \qquad Q \leq E-08 \tag{23}$$

where P denotes the constraint error and Q denotes the error in the optimality conditions.

The results are given in Fig. 4, which contains six parts: the wind velocity components W_x, W_h, the flight altitude h, the relative velocity V, the relative path inclination γ, the relative angle of attack α, and the absolute path inclination γ_e. The following comments are pertinent.

Altitude

For all the optimal trajectories, the altitude distribution $h(t)$ exhibits a monotonic behavior, regardless of the windshear model. For model WS2, the function $h(t)$ is almost identical with that characterizing the nominal trajectory in the absence of downdraft. This means that $\gamma_e \cong \gamma_{e0}$, a condition which can be achieved by properly adjusting the angle of attack $\alpha(t)$.

For model WS3, there is a large time interval, approximately $\Delta t = 18$ s, in which the optimal trajectory is nearly horizontal ($\gamma_e \cong 0$); this is due to the combined effect of the horizontal shear and the downdraft. After passing through the shear region, the aircraft resumes climbing. For model WS1, the function $h(t)$ is intermediate between that of model WS2 and that of model WS3, being closer to the latter than to the former.

Angle of Attack

For model WS2, a gradual, moderate change in the angle of attack is required in order to compensate for the downdraft. However, the angle-of-attack boundary is never reached. This is why, by properly adjusting the angle-of-attack distribution $\alpha(t)$, one can obtain an optimal trajectory close to the nominal trajectory in the absence of downdraft.

For models WS1 and WS3, an initial decrease in the angle of attack is needed, followed by a gradual, sustained increase until the angle-of-attack boundary is reached. This occurs at about the time when the shear ends ($t = 18$ s). Afterward, the angle of attack is kept at the maximum permissible value for a relatively long time interval ($\Delta t = 10$ s). As a consequence, for both models WS1 and WS3, the optimal trajectory departs to a considerable extent from the nominal trajectory.

It is interesting to note that the angle-of-attack distributions of models WS1 and WS3 are nearly the same, which means that the control action is mostly determined by the horizontal shear. This also means that the effect of the downdraft is mostly kinematical rather than dynamical: the function $h(t)$ for model WS3 is shifted downward with respect to that for model WS1.

Absolute Path Inclination

For model WS2, the optimal trajectory is such that $\gamma_e \cong \gamma_{e0}$. Hence, the performance index of Problem (P), minimax $|\Delta\gamma_e|$, is nearly zero.

For models WS1 and WS3, the behavior of γ_e is quite different. Initially γ_e must be decreased until a certain critical value $\gamma_e = \gamma_{ec}$ is reached; then, this value is nearly maintained for a relatively long time interval ($\Delta t = 24$ s for model WS1 and $\Delta t = 18$ s for model WS3). After passing through the shear region, the value of γ_e is gradually increased to $\gamma_e \cong \gamma_{e0}$.

The critical value of the absolute path inclination is of interest in constructing a guidance algorithm. From the inspection of the optimal trajectories, we see that $\gamma_{ec}/\gamma_{e0} \cong 1$ for model WS2, $\gamma_{ec}/\gamma_{e0} \cong 0.4$ for model WS1, and $\gamma_{ec}/\gamma_{e0} \cong 0$ for model WS3.

Relative Path Inclination

For model WS1, the relative path inclination γ behaves in about the same way as the absolute path inclination γ_e. This is due to the absence of downdraft.

For models WS2 and WS3, the relative path inclination γ is larger than the absolute path inclination γ_e. This is in order to compensate for the presence of downdraft.

Relative Velocity

For model WS2, there is a mild decrease in relative velocity, consistent with the increase in the angle of attack. The velocity decrease ends at about the time when the downdraft ends.

For models WS1 and WS3, there is a stronger decrease in relative velocity. The maximum drop in relative velocity occurs at about the time when the shear ends ($t = 18$ s).

Comment

From the present study of optimal trajectories (Fig. 4) as well as from previous studies (Refs. 2–4), the following conclusions can be inferred. For weak-to-moderate shear/downdraft combinations, the optimal trajectory is characterized by a monotonic climb. For severe shear/downdraft combinations, the optimal trajectory is characterized by an initial climb, followed by nearly-horizontal flight, followed by renewed climbing after the aircraft has passed through the shear region.

IV. Acceleration Guidance

In this section, we present a guidance scheme based on relative acceleration. Its objective is to approximate the behavior of the optimal trajectories in a windshear. The guidance scheme relies on the fact that, for the windshear portion of the

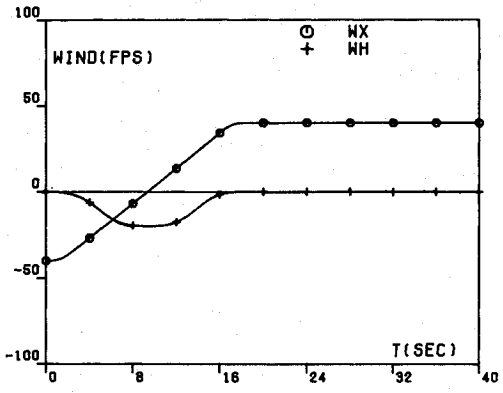

Fig. 4a Optimal trajectory: wind velocity components W_x, W_h vs time t.

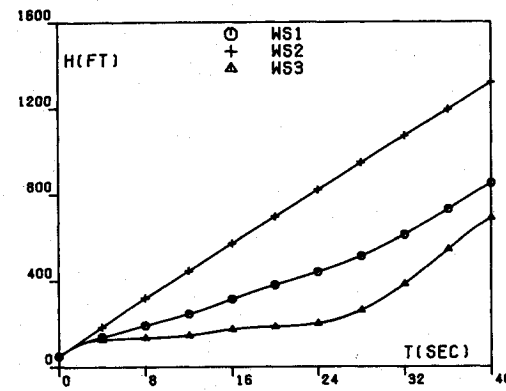

Fig. 4b Optimal trajectory: altitude h vs time t.

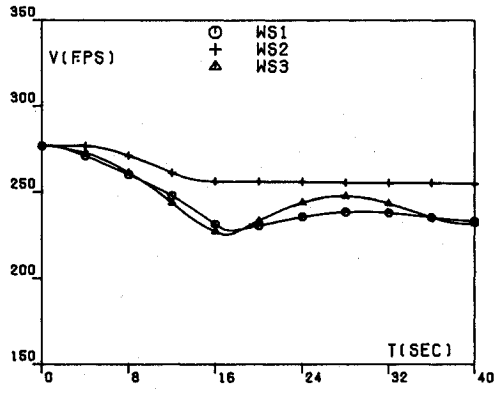

Fig. 4c Optimal trajectory: relative velocity V vs time t.

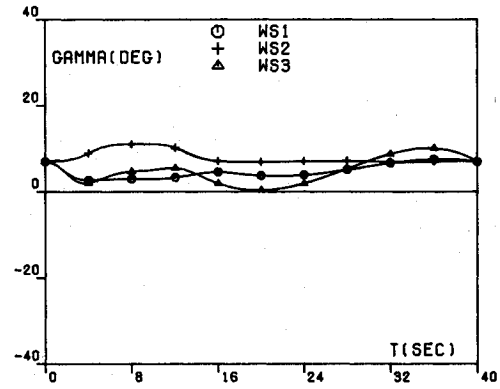

Fig. 4d Optimal trajectory: relative path inclination γ vs time t.

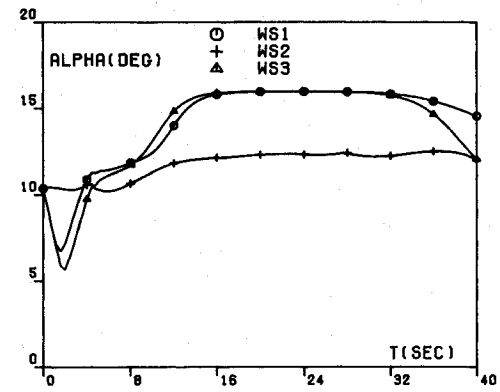

Fig. 4e Optimal trajectory: relative angle of attack α vs time t.

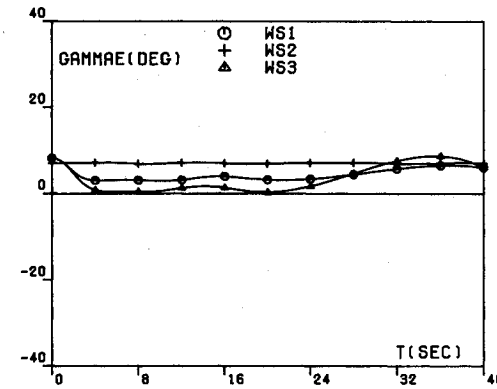

Fig. 4f Optimal trajectory: absolute path inclination γ_e vs time t.

flight, the relative acceleration is approximately proportional to the shear/downdraft factor F defined in this section.

We consider the equations of motion in the form of Eqs. (1) and (2). Upon combining Eqs. (1b) and (2a), we obtain the relation

$$\dot{V}/g + \dot{h}/V - (T/W)\cos(\alpha+\delta) + D/W + (\dot{W}_x/g)\cos\gamma + (\dot{W}_h/g)\sin\gamma - W_h/V = 0 \tag{24}$$

which can be rewritten in the form

$$\dot{V}/g + (\dot{h} - \dot{h}_*)/V + F = 0 \tag{25}$$

where

$$\dot{h}_*/V = (T/W)\cos(\alpha+\delta) - D/W \tag{26a}$$

$$F = (\dot{W}_x/g)\cos\gamma + (\dot{W}_h/g)\sin\gamma - W_h/V \tag{26b}$$

The interpretation of Eq. (25) is as follows: the first term is the relative acceleration expressed in terms of the acceleration of gravity, the second term expresses the deviation of the rate of climb from its instantaneous quasi-steady value in the absence of shear and downdraft, and the third term is the shear/downdraft factor, which combines the effects of the shear and the downdraft into a single entity.

The acceleration guidance law is based on the assumption of proportionality between the first term and the third term in Eq. (25), namely,

$$\dot{V}/g + CF = 0 \tag{27a}$$

with the implication that

$$(\dot{h} - \dot{h}_*)/V + (1-C)F = 0 \tag{27b}$$

where C is a dimensionless constant. Note that Eqs. (27) are consistent with Eq. (25) for any value of the constant C.

The proportionality assumption is suggested by a detailed analysis of the optimal trajectories of Fig. 4. From this analysis, it appears that the most desirable value of the constant C is

$$C = 0.50 \tag{28}$$

The acceleration guidance law can be implemented in either analytical or feedback control form. This is done in the following sections.

A. Analytical Form

Upon combining Eqs. (1), (2), (26), and (27) and upon eliminating the time derivatives of the state variables, we obtain the following relation:

$$(T/W)\cos(\alpha+\delta) - D/W - \sin\gamma - G = 0 \tag{29a}$$

where

$$G = (1-C)\left[(\dot{W}_x/g)\cos\gamma + (\dot{W}_h/g)\sin\gamma\right] + C(W_h/V) \tag{29b}$$

which supplies implicitly the angle of attack α in terms of the state variables and the modified shear/downdraft factor G.

Next, we employ the representation (9) for the thrust and the representation (10) for the drag, and we expand the trigonometric term $\cos(\alpha+\delta)$ in a Taylor series as follows:

$$\cos(\alpha+\delta) \cong 1 - (1/2)(\alpha+\delta)^2 \tag{30}$$

Therefore, from Eq. (29a) we obtain the following quadratic equation:

$$H_0 + H_1\alpha + H_2\alpha^2 = 0, \qquad \alpha \le \alpha_* \tag{31}$$

which admits the solution

$$\alpha = (1/2H_2)\left[-H_1 + \sqrt{(H_1^2 - 4H_0H_2)}\right], \qquad \alpha \le \alpha_* \tag{32}$$

The coefficients H_0, H_1, and H_2 depend on the state variables and the modified shear/downdraft factor G. They are given by

$$H_0 = \left[(-2+\delta^2)/2mg\right](A_0 + A_1V + A_2V^2) + (B_0\rho S/2mg)V^2 + \sin\gamma + G \tag{33a}$$

$$H_1 = (\delta/mg)(A_0 + A_1V + A_2V^2) + (B_1\rho S/2mg)V^2 \tag{33b}$$

$$H_2 = (1/2mg)(A_0 + A_1V + A_2V^2) + (B_2\rho S/2mg)V^2 \tag{33c}$$

Equation (32) in conjunction with Eqs. (33) supplies explicitly the angle of attack α in terms of the state variables and the modified shear/downdraft factor G.

B. Feedback Control Form

Alternatively, Eq. (27a) can be implemented through the feedback control law

$$\alpha - \tilde{\alpha}(V) = -K(-\dot{V}/g - CF), \qquad \alpha \le \alpha_* \tag{34}$$

where K is the gain coefficient. In Eq. (34), $\tilde{\alpha}(V)$ denotes the nominal angle of attack whose conception is now discussed.

Nominal Angle of Attack

From the analysis of the optimal trajectories of Fig. 4, it appears that there is some relation between the angle of attack and the velocity; it also appears that this relation is relatively insensitive to the windshear model and intensity. More specifically, low angles of attack correspond to high velocities, and high angles of attack correspond to low velocities. An analytical form for the function $\tilde{\alpha}(V)$ is derived here.

Recall Eq. (2b), and assume that, along a large portion of the optimal trajectory,

$$\cos\gamma \cong 1, \qquad \sin\gamma \cong \gamma \tag{35a}$$

$$|\dot{W}_x\gamma/g| \ll 1, \qquad |\dot{W}_h/g| \ll 1, \qquad |V\dot{\gamma}/g| \ll 1 \tag{35b}$$

Under these conditions, Eq. (2b) yields the following nondifferential equation:

$$(T/W)\sin(\alpha+\delta) + L/W - 1 = 0 \tag{36}$$

which supplies implicitly the function $\tilde{\alpha}(V)$.

Next, we employ the representation (9) for the thrust and the representation (11) for the lift, and we expand the trigonometric term $\sin(\alpha+\delta)$ in a Taylor series as follows:

$$\sin(\alpha+\delta) \cong (\alpha+\delta) \tag{37}$$

Therefore, from Eq. (36), we obtain the following algebraic equations:

$$D_0 + D_1\alpha = 0, \qquad \alpha \le \alpha_{**} \tag{38a}$$

$$E_0 + E_1(\alpha - \alpha_{**}) + E_2(\alpha - \alpha_{**})^2 = 0, \qquad \alpha_{**} \le \alpha \le \alpha_* \tag{38b}$$

which admit the solutions

$$\alpha = -D_0/D_1, \qquad \alpha \le \alpha_{**} \tag{39a}$$

$$\alpha = \alpha_{**} + (1/2E_2)\left[-E_1 + \sqrt{(E_1^2 - 4E_0E_2)}\right], \qquad \alpha_{**} \le \alpha \le \alpha_* \tag{39b}$$

The coefficients D_0, D_1, E_0, E_1, and E_2 depend on the velocity. They are given by

$$D_0 = -1 + (\delta/mg)(A_0 + A_1V + A_2V^2) + (C_0\rho S/2mg)V^2 \tag{40a}$$

$$D_1 = (1/mg)(A_0 + A_1V + A_2V^2) + (C_1\rho S/2mg)V^2 \tag{40b}$$

and

$$E_0 = D_0 + D_1\alpha_{**} \tag{41a}$$

$$E_1 = D_1 \tag{41b}$$

$$E_2 = (C_2\rho S/2mg)V^2 \tag{41c}$$

Equations (39) in conjunction with Eqs. (40) and (41) supply explicitly the function $\tilde{\alpha}(V)$.

C. Data for the Examples

The data for the examples are the same as those of Sec. IIID. In particular, the initial conditions are given by Eqs. (19a) and (19b) and the final time is given by Eq. (21). The angle of attack is subject to Ineq. (7a), with $\alpha_* = 16$ deg.

Windshear models WS1, WS2, and WS3 are considered. The acceleration guidance scheme is implemented using both the analytical form (32) with $C = 0.50$ and the feedback con-

trol form (34) with $C = 0.50$ and $K = 10$. However, the computations presented here refer to the analytical form (32).

D. Numerical Results

The numerical results are given in Fig. 5, which contains six parts: the wind velocity components W_x, W_h, the flight altitude h, the relative velocity V, the relative path inclination γ, the relative angle of attack α, and the absolute path inclination γ_e. Comparison of Figs. 4 and 5 shows that there is a remarkable qualitative agreement between the acceleration guidance trajectories and the optimal trajectories. In particular, the following points must be noted.

Altitude

For model WS2, the function $h(t)$ of the acceleration guidance trajectory (AGT) is almost identical with the function $h(t)$ characterizing the nominal trajectory in the absence of downdraft; therefore, it behaves as the function $h(t)$ of the optimal trajectory (OT). For model WS3, the AGT has a slight dip with respect to the local horizon; it is close to the OT, which is nearly horizontal, but without a dip. For model WS1, the function $h(t)$ of the AGT is intermediate between that of model WS2 and that of model WS3, being closer to the latter than to the former; therefore, it behaves as the function $h(t)$ of the OT.

Angle of Attack

For model WS2, the AGT exhibits a gradual, moderate change in the angle of attack. The angle-of-attack boundary is never reached; hence, the function $\alpha(t)$ of the AGT behaves as the function $\alpha(t)$ of the OT.

For models WS1 and WS3, the AGT exhibits an initial decrease in the angle of attack, followed by a gradual, sustained increase; the angle-of-attack boundary is reached at

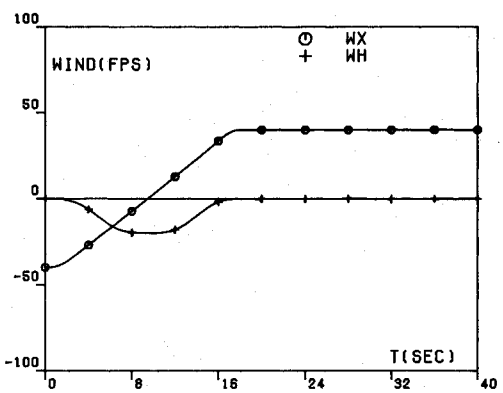

Fig. 5a Acceleration guidance: wind velocity components W_x, W_h vs time t.

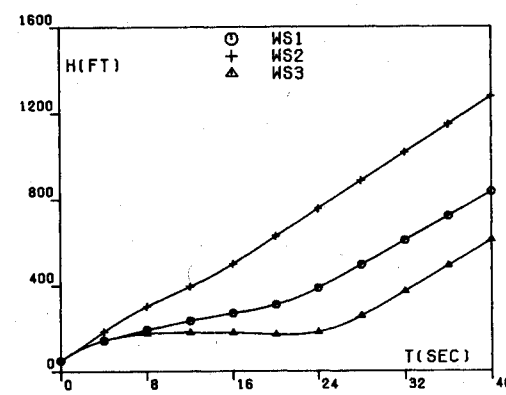

Fig. 5b Acceleration guidance: altitude h vs time t.

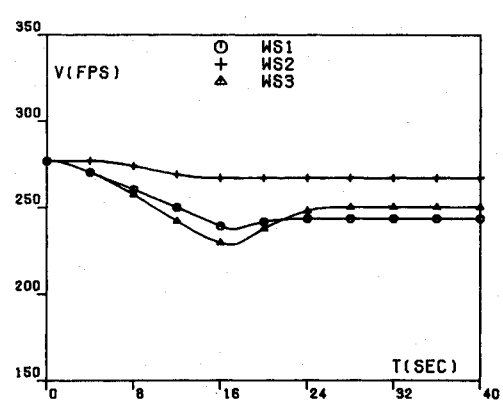

Fig. 5c Acceleration guidance: relative velocity V vs time t.

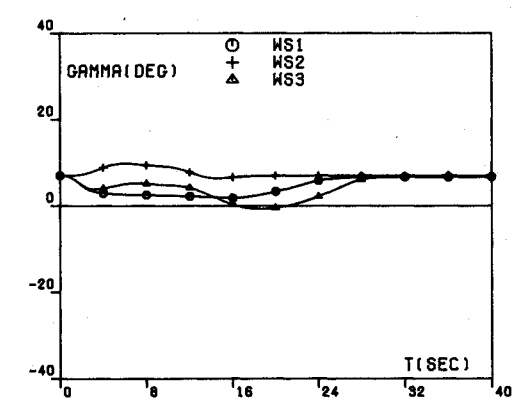

Fig. 5d Acceleration guidance: relative path inclination γ vs time t.

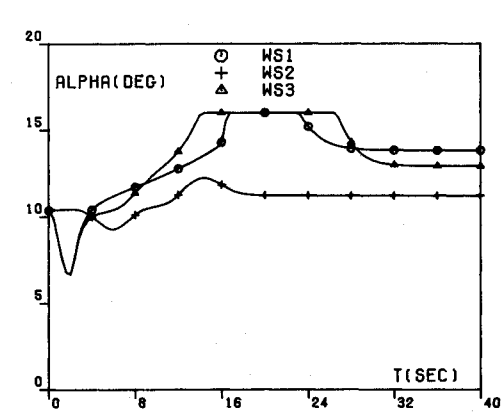

Fig. 5e Acceleration guidance: relative angle of attack α vs time t.

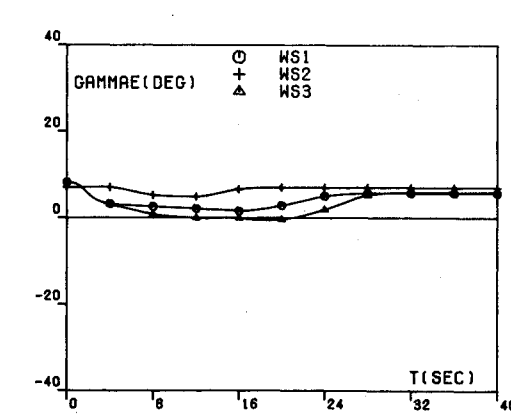

Fig. 5f Acceleration guidance: absolute path inclination γ_e vs time t.

about the time when the shear ends. Once more, the function $\alpha(t)$ of the AGT behaves as the function $\alpha(t)$ of the OT.

Absolute Path Inclination

For model WS2, the AGT is such that $\gamma_e \cong \gamma_{e0}$; this property is consistent with the analogous property of the OT. For models WS1 and WS3, the absolute path inclination γ_e of the AGT decreases until a certain critical value $\gamma_e = \gamma_{ec}$ is reached; then, this value is nearly maintained for a relatively long time interval. After passing through the shear region, the value of γ_e is gradually increased to $\gamma_e \cong \gamma_{e0}$. Once more, this property is consistent with the analogous property of the OT.

Relative Path Inclination

For model WS1, the relative path inclination γ of the AGT behaves in about the same way as the absolute path inclination γ_e. This property is consistent with the analogous property of the OT.

For models WS2 and WS3, the relative path inclination γ of the AGT is larger than the absolute path inclination γ_e. Once more, this property is consistent with the analogous property of the OT.

Relative Velocity

For model WS2, the AGT exhibits a mild decrease in relative velocity. The velocity decrease ends at about the time when the downdraft ends. This property is consistent with the analogous property of the OT.

For models WS1 and WS3, the AGT exhibits a stronger decrease in relative velocity. The maximum drop in relative velocity occurs at about the time when the shear ends. Once more, this property is consistent with the analogous property of the OT.

Comment

From the present study of acceleration guidance trajectories (Fig. 5) as well as from previous studies (Refs. 5 and 6), the following conclusions can be inferred. For weak-to-moderate shear/downdraft combinations, the AGT is characterized by a monotonic climb. For severe shear/downdraft combinations, the AGT is characterized by an initial climb, followed by nearly-horizontal flight, followed by renewed climbing after the aircraft has passed through the shear region. These properties are consistent with the analogous properties of the OT.

V. Conclusions

This paper is concerned with guidance strategies for near-optimum performance in a windshear. The takeoff problem is considered with reference to flight in a vertical plane. In addition to the horizontal shear, the presence of a downdraft is assumed.

First, trajectories for optimum performance in a windshear are determined for different windshear models and different windshear intensities. In this approach, global information on the wind flowfield is needed. Numerical experiments with the optimal control approach lead to the following conclusions: (1) for weak-to-moderate shear/downdraft combinations, the optimal trajectory is characterized by a monotonic climb, and (2) for severe shear/downdraft combinations, the optimal trajectory is characterized by an initial climb, followed by nearly-horizontal flight, followed by renewed climbing after the aircraft has passed through the shear region.

Then, guidance strategies for near-optimum performance in a windshear are developed, starting from the optimal trajectories. Specifically, an acceleration guidance scheme based on the relative acceleration is presented in both analytical and feedback control forms. In this approach, local information on the wind flowfield is needed.

Numerical experiments with the acceleration guidance scheme show that this scheme preserves the two previously mentioned properties of the optimal trajectories. Not only are the resulting trajectories close to the optimum trajectories, but they are superior to the trajectories arising from alternative guidance schemes (see Ref. 5, Part 2).

An important characteristic of the acceleration guidance scheme is its simplicity. Indeed, this guidance scheme is implementable if local information on the windshear, the downdraft, and the state of the aircraft is available.

Acknowledgments

This research was supported by the NASA Langley Research Center, Grant NAG-1-516, and by the Boeing Commercial Airplane Company. The authors are indebted to Dr. R.L. Bowles of the NASA Langley Research Center for helpful discussions. The authors are also indebted to Mr. Z.G. Zhao and Mr. E. Kamaric of Rice University for analytical and computational assistance.

References

[1]Miele, A., Wang, T., and Melvin, W.W., "Optimization and Acceleration Guidance of Flight Trajectories in a Windshear," AIAA Paper 86-2036, 1986.

[2]Miele, A., Wang, T., and Melvin, W.W., "Optimal Flight Trajectories in the Presence of Windshear, Parts 1–4," Aero-Astronautics Repts. 191–194, Rice University, 1985.

[3]Miele, A., "Summary Report on NASA Grant No. NAG-1-516, Optimal Flight Trajectories in the Presence of Windshear, 1984–85," Aero-Astronautics Rept. 195, Rice University, 1985.

[4]Miele, A., Wang, T., and Melvin, W.W, "Optimal Take-Off Trajectories in the Presence of Windshear," *Journal of Optimization Theory and Applications*, Vol. 49, April 1986, pp. 1–45.

[5]Miele, A., Wang, T., and Melvin, W.W., "Guidance Strategies for Near-Optimum Performance in a Windshear, Parts 1–2," Aero-Astronautics Repts. 201–202, Rice University, 1986.

[6]Miele, A., Wang, T., and Melvin, W.W., "Guidance Strategies for Near-Optimum Take-Off Performance in a Windshear," *Journal of Optimization Theory and Applications*, Vol. 50, July 1986, pp. 1–47.

[7]Anonymous, N.N., *Low Altitude Windshear and Its Hazard to Aviation*, National Academy Press, Washington, DC, 1983.

[8]Miele, A., *Flight Mechanics, Vol. 1, Theory of Flight Paths*, Addison-Wesley, Reading, MA, 1962.

[9]Frost, W. and Bowles, R.L., "Windshear Terms in the Equations of Aircraft Motion," *Journal of Aircraft*, Vol. 21, Nov. 1984, pp. 866–872.

[10]Alexander, M.B. and Camp, D.W., "Wind Speed and Direction Shears with Associated Vertical Motion during Strong Surface Winds," NASA, TM 82566, 1984.

[11]Frost, W., Chang, H.P., Elmore, K.L., and McCarthy, J., "Simulated Flight through JAWS Windshear: In-Depth Analysis Results, AIAA Paper 84-0276, 1984.

[12]Campbell, C.W., "A Spatial Model of Windshear and Turbulence for Flight Simulation," NASA, TP 2313, 1984.

[13]Leitmann, G., *The Calculus of Variations and Optimal Control*, Plenum, New York, NY, 1981.

[14]Miele, A., Pritchard, R.E., and Damoulakis, J.N., "Sequential Gradient-Restoration Algorithm for Optimal Control Problems," *Journal of Optimization Theory and Applications*, Vol. 5, April 1970, pp. 235–282.

[15]Miele, A., Damoulakis, J.N., Cloutier, J.R., and Tietze, J.L., "Sequential Gradient-Restoration Algorithm for Optimal Control Problems with Nondifferential Constraints," *Journal of Optimization Theory and Applications*, Vol. 13, Feb. 1974, pp. 218–255.

[16]Miele, A. and Wang, T., "Primal-Dual Properties of Sequential Gradient-Restoration Algorithms for Optimal Control Problems, Part 1, Basic Problem," *Integral Methods in Science and Engineering*, edited by F.R. Payne, Hemisphere, Washington, DC, 1986, pp. 577–607.

[17]Miele, A. and Wang, T., "Primal-Dual Properties of Sequential Gradient-Restoration Algorithms for Optimal Control Problems, Part

2, General Problem," *Journal of Mathematical Analysis and Applications*, Vol. 119, Oct.–Nov. 1986, pp. 21–54.

[18]Michael, G.J., "Computation of Chebyshev Optimal Control," *AIAA Journal*, Vol. 9, May 1971, pp. 973–975.

[19]Miele, A. and Wang, T., "An Elementary Proof of a Functional Analysis Result Having Interest for Minimax Optimal Control of Aeroassisted Orbital Transfer Vehicles," Aero-Astronautics Rept. 182, Rice University, 1985.

[20]Anonymous, N.N., "Flight Path Control in Windshear," *Boeing Airliner*, Jan.–March 1985, pp. 1–12.

[21]Psiaki, M.L. and Stengel, R.F., "Analysis of Aircraft Control Strategies for Microburst Encounter," AIAA Paper 84-0238, 1984.

[22]Psiaki, M.L. and Stengel, R.F., "Optimal Flight Paths through Microburst Wind Profiles," *Journal of Aircraft*, Vol. 23, Aug. 1986, pp. 629–635.

[23]Miele, A., Wang, T., and Melvin, W.W., "Optimization and Gamma/Theta Guidance of Flight Trajectories in a Windshear," ICAS Paper 86-564, 15th Congress of the International Council of the Aeronautical Sciences, London, England, 1986.

[24]Miele, A., Wang, T., and Melvin, W.W., "Quasi-Steady Flight to Quasi-Steady Flight Transition in a Windshear: Trajectory Optimization," 6th IFAC Workshop on Control Applications of Nonlinear Programming and Optimization, London, England, 1986.

[25]Miele, A., "Quasi-Steady Flight to Quasi-Steady Flight Transition in a Windshear: Trajectory Guidance," AIAA Paper 87-0271, 1987.